

Virtual Institute of Physics

## Errata

The editor would like to announce the retraction of this paper from Digest Journal of Nanomaterials and Biostructures for the reason of research misconduct.

The paper has been submitted for publication without the consensus of all named authors. Also, it has been brought to our attention that there is a conflict between authors that lead to immoral behavior concerning stolen data between authors.

The editorial staff of the journal would like to apologize for the misunderstanding and technical error that led to the publication of the article in this journal.

Managing Editor

Dr. Iosif - Daniel Șimăndan

A handwritten signature in blue ink, consisting of a stylized, cursive representation of the letters "I" and "D".

## Shape- and area-controlled growth of Cu particles during electrodeposition

B. S Yang<sup>a</sup>, Y. Ai<sup>b</sup>, X. Z. Zhan<sup>c</sup>, X. W. Liu<sup>a,\*</sup>

<sup>a</sup>*Institute of Technological Sciences, Wuhan University, Wuhan 430072, China*

<sup>b</sup>*School of Mechanical Science & Engineering, Huazhong University of Science and Technology, Wuhan 430074, China*

<sup>c</sup>*School of Power and Mechanical Engineering, Wuhan University, Wuhan 430072, China*

Shape-controlled growth (leaf-like, dendritic, flower-like, multi-corner and multi-edge) and area-controlled growth (island- and linear-) of Cu particles during a simple electrodeposition were reported. Defects and types of substrates play a major role in the preparation process, furthermore temperature and ultrasonic vibration of electrolyte. The series of well-shaped Cu particles were fabricated through changing substrates (iron, graphite or copper sheets) and electrolyte temperature (50°C, 70°C and 80°C), or introducing ultrasonic vibration, endowing Cu materials with intriguing properties such as an increased surface area and active site for SERS. By introducing two kinds of linear-defects (20~40 μm and 5 μm width) on the substrate, the selective electrodeposition phenomena appeared: island-controlled growth and linear-controlled growth.

(Received August 3, 2021; Accepted November 2, 2021)

*Keywords:* Electrodeposition, Area-controlled growth, Shape-controlled growth, Substrate, Defect, Copper

### 1. Introduction

Nowadays, continuously growing attention are paid to explore Cu particles with a variety of specific shapes and structures to exert advantages in electricity, light, thermal conductivity, catalysis etc. [1-3]. Many morphologies and structures have been successfully discovered, including one-dimensional wires and rods, two-dimensional flakes, three-dimensional polyhedrons, spheres, and various other geometric shapes [4-6]. Fractal or branched structure like leaf-like, dendritic and flower-like have also been successfully synthesized by several methods such as hydrothermal method, reduction method, vapor deposition method, magnetron sputtering method etc. [7,8]. However, most of them have high requirements for special advanced equipment, high temperature, the presence of organic additives, long experimental periods or environmental pollution [9]. For example, Quang Duc Truong et al reported the synthesis of unusual cross-linked hyperbranched copper dendrites using copper oxalate complex as a precursor [10].

Electrodeposition is an alternative method due to several advantages: low power consumption, potential of synthesizing particles with various size and shape by changing electrolysis parameters such as: type and composition of electrolytes, temperature, voltage or current, electrolysis time etc. [11-17]. For parameters like type and composition of electrolytes or temperature, many related studies have successfully prepared crystals of different sizes and shapes [18,19]. To date, there also have been many reports on the synthesis of metal particles with fractal or branched structure especially dendrites by electrodeposition [20,21]. However, the types of structures prepared are very limited, usually only leaf-like or dendritic and don't have very obvious bionic structures like leaf or flower, there are more interesting fractal or branch structures like flower worth exploring.

The influence of growth substrate (electrode) with different composition or crystal orientation on the morphology and size of the product has been studied, but the types of products are not rich [22]. There are still more to explore. To the best of our knowledge, there are existing discussions about 3D island growth for nuclei form and coalesce [23-25]. But substrate effects on particle nucleation and distribution have rarely been deeply reported [26,27]. It is also meaningful to investigate this area by introducing some defects on substrate, observing whether lead to new phenomena. [28].

\*Corresponding author: 2019206520004@whu.edu.cn

Here, a series of Cu particles with fractal or branched structures including leaf-like, dendritic, flower-like, multi-corner and multi-edge are obtained in a simple electrodeposition by changing substrates, temperature or introducing ultrasonic vibration, without template and surfactant. It was perhaps the first time for part of the structures to be reported or synthesized by such a simple electrodeposition method. The controlled growth in selective area were also reported and further confirmed by Ni particles under the same treatment. The influence of substrate defects (concave grooves) with width of 20~40  $\mu\text{m}$  and 5  $\mu\text{m}$  on the growth distribution were studied respectively. The distribution, shape and surface morphology were characterized by scanning electron microscopy (SEM), including the leaf-like, dendritic, flower-like, multi-corner and multi-edge particles and linear-controlled distribution on the defected area of substrates. The crystal structure and composition were further studied by transmission electron microscope (TEM), UV-Vis and X-ray diffraction pattern (XRD).

## 2. Experimental

### 2.1. Reagent

All reagents used in this work were analytical grade, including  $\text{CuSO}_4 \cdot 5\text{H}_2\text{O}$  as a  $\text{Cu}^{2+}$  source,  $\text{NiSO}_4 \cdot 6\text{H}_2\text{O}$  as a  $\text{Ni}^{2+}$  source,  $\text{NaCl}$ ,  $\text{H}_3\text{BO}_3$ , anhydrous ethanol and hydrochloric acid were obtained from Sinopharm Chemical Reagent Co. Ltd., China. The electrolyte solution A was prepared for synthesizing Cu crystals, where  $\text{CuSO}_4 \cdot 5\text{H}_2\text{O}$  (50g/L) was dissolved in deionized water. The electrolyte solution B for Ni crystals synthesis was composed of  $\text{NiSO}_4 \cdot 6\text{H}_2\text{O}$  (300 g/L),  $\text{NaCl}$  (40 g/L) and  $\text{H}_3\text{BO}_3$  (40 g/L).

### 2.2. Electrodeposition

As shown in Fig.1.a, the electrodeposition process was carried out in the two-electrode battery. Highly purified sheets (iron, graphite and copper) with diameter of 10mm and thickness of 3mm were used as the cathodic growth substrate. Steel needle (diameter 1mm, length 20mm) was positioned at a distance of ~5 mm from the upper surface of cathodic substrate, connected with the positive electrode as anode substrate. The voltage was set as 18 V and the temperature of electrolyte was maintained at 30  $^\circ\text{C}$ , 50 $^\circ\text{C}$ , 70 $^\circ\text{C}$  and 80 $^\circ\text{C}$  by heating in a water bath.

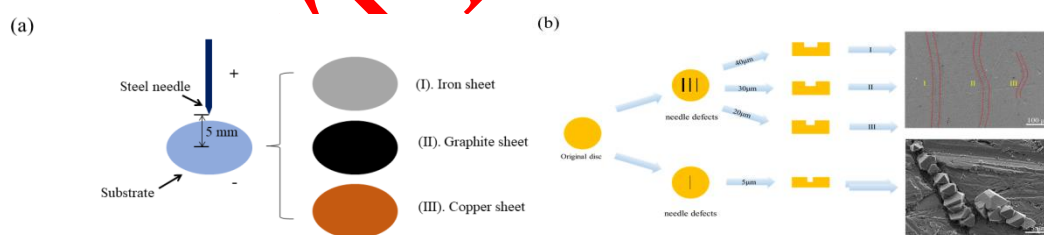


Fig.1. Diagram of the electrodeposition with cathodic substrates of different materials and defects.

Prior to electrodeposition, one side of the substrate was mechanically polished using silicon carbide papers of grit #400 up to #7000, then scratched by thin steel needles to obtain linear defects (concave grooves) with different width on surface (40  $\mu\text{m}$ , 30  $\mu\text{m}$ , 20  $\mu\text{m}$  and 5  $\mu\text{m}$ ), cleaned with ethanol to remove oil and impurities on the surface, ultrasonically cleaned in acetone, dried in the air.

### 2.3. Characterization

SEM images obtained by MIRA 3 LMH at 5 kV were used for the morphological and distribution characterization. Shape-controlled particles were mechanically peeled off from electrode, dispersed in absolute ethanol and dropped on aluminum foil, while distribution-controlled were observed particle distribution directly on the substrates. TEM and SAED images obtained by JEOL 2100 at 200 kV were used for the crystal structure analysis. The samples were made by the

same suspension used in SEM on a 200 mesh carbon-coated Cu grid and then drying in air. Centrifuge and dry the suspension to obtain Cu powder for XRD and SERS. The XRD spectra were recorded using a Bruker D8 X-ray diffractometer (Cu  $K\alpha$  source) with a  $2\theta$  range of  $10^\circ$  to  $80^\circ$ . UV-Vis characterization (UV-2550, Shimadzu) was carried out on dispersions. Rhodamine 6 G (R6G) dye molecules was used for SERS characterization (Renishaw inVia, 532 nm) to explore enhancement effects. Among them, the components of each group of samples were: ( I ) 10 mg R6G and 1 mg leaf-like; ( II ) 10 mg R6G and 1 mg flower-like; ( III ) 1 mg pure R6G.

### 3. Results and Discussion

#### 3.1. Shape-controlled analysis

Similar to branches and leaves in nature, Cu particles obtained on steel needle, iron sheet and copper sheet at  $50^\circ\text{C}$  and  $80^\circ\text{C}$  have structures of both "leaves" and "petioles", which are composed of units of different shapes (Fig.2).

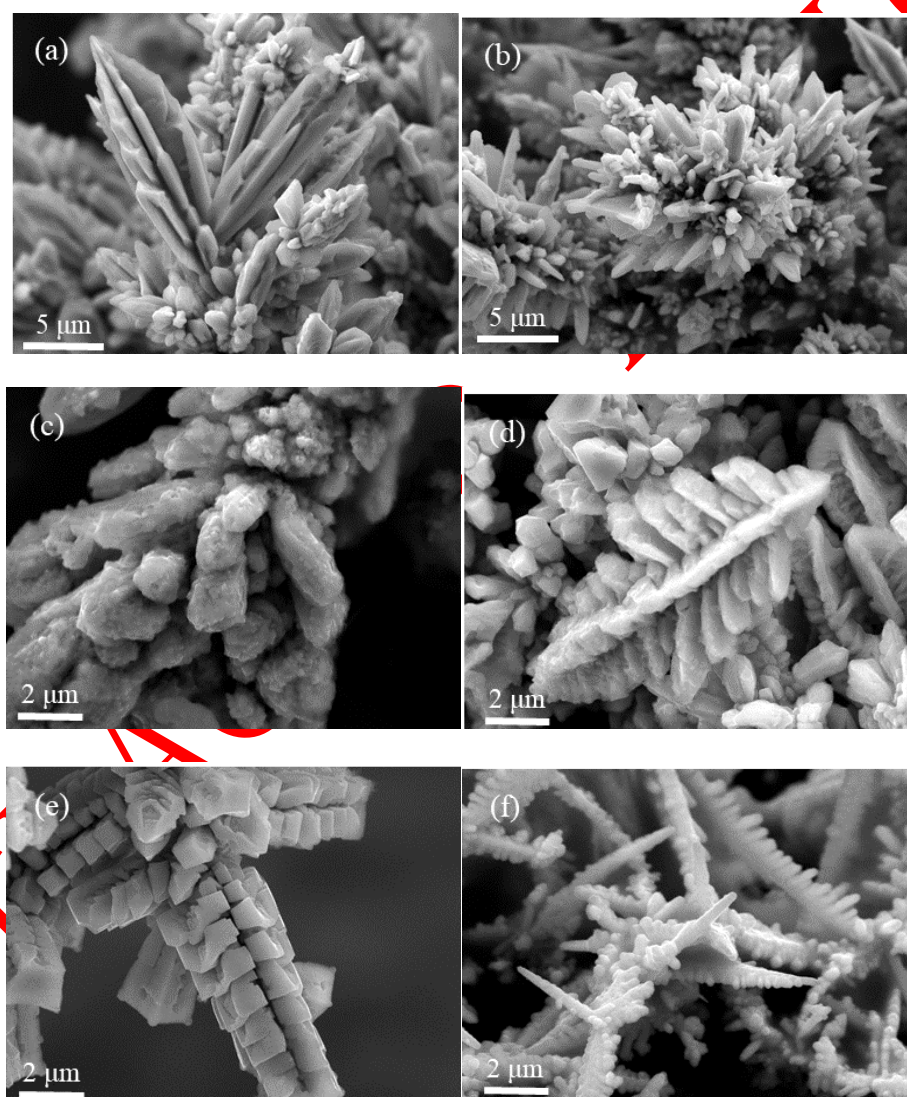


Fig.2. SEM characterization leaf-like and dendritic Cu particles

It can be clearly seen in Fig. 2a and b that the use of steel needle as the substrate is more conducive to the formation of needle-leaf particles. The length of needle leaves are up to  $1\sim 3\ \mu\text{m}$  at  $50^\circ\text{C}$  and  $0.5\sim 1\ \mu\text{m}$  at  $80^\circ\text{C}$ , respectively. In Fig. 2c and d, it is observed that on the substrate of iron sheet the dendrites appear and have a more dispersed and significant branch structure. The leaves are

symmetrically distributed around the branches with diameters of 1~2  $\mu\text{m}$ , and the angle between the branches is almost the same as  $\sim 60^\circ$ . When the substrate is selected as copper sheet, dendrites more similar to knuckles or spurs were found in Fig.2e and f, respectively.

At the same time, the overall size of the particles from 50°C (Fig.2 a, c and e) to 80 °C (Fig.2 b, d and f) also conforms to the regular rule in electrodeposition process that the higher the temperature, the smaller and thinner the products are.

It can be seen from Fig. 3a that 3D flower-like Cu particles grow on the graphite sheet at 70°C, which is composed of a large number of ultra-thin nanosheets with a thickness of only tens of nanometers, and the overall component units are relatively uniform. Fig. 3b shows that the nanosheets begin to become diverse in shape on the iron needle at 70°C, but in the end it magically constitutes a flower-shaped particle with more bionic characteristics. For these two kinds of nanosheets-composed flower-like particles, when light waves irradiate the surface of the nanosheets, multiple reflections will occur between the sheets, which greatly increases the absorption and utilization of light, just like the study in Au nanoplates accomplished by Taekyung Yu et al [29]. Fig 3c and d show Cu particles with multi edges and corners on the graphite sheet and copper sheet when furtherly vibrating the electrolyte by ultrasonic at 70°C. In Fig. 3c, it can be seen that there are many excess edges formed on some cube-shaped Cu particles, and some even as many as 5~10. Similarly, some extra small corners have grown on some polyhedral Cu particles with the number and size of 4~6, 0.2 $\mu\text{m}$  ~0.8 $\mu\text{m}$ , respectively (Fig. 3d). The larger specific surface area brought by the extra edges and corners is also more conducive to the adsorption and catalysis.

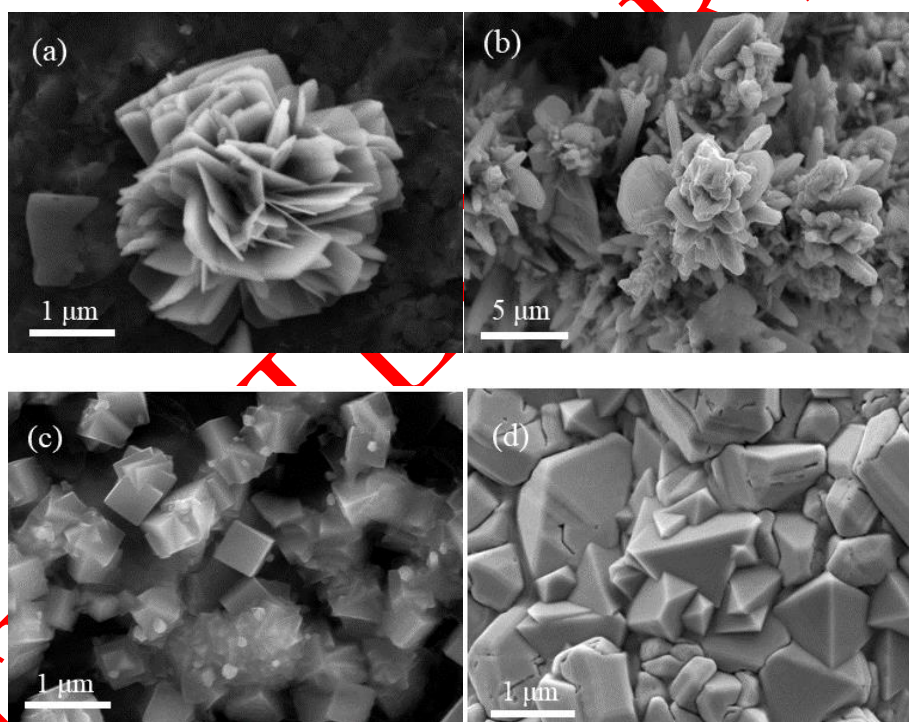


Fig. 3. SEM characterizations of flower-like, multi-corner and multi-edge Cu particles.

In order to furtherly confirm the structure and composition of Cu particles, the dendrites and flower-like particles in Fig. 2a and Fig. 3a were selected for TEM characterization. Fig. 4a and d show the morphologies of Cu blades and Cu nanosheets at low magnification, respectively. In addition, the diffraction ring of Fig. 4b indicate that the blades are composed of many crystal grains. While the single crystal diffraction spots in Fig. 4e indicate that the nanosheets are single crystals and have good crystallinity. Fig. 4c and f show Cu crystals in high resolution mode and demonstrate the regular lattice planes of 2.088 Å is consistent with the (111) plane of FCC Cu (JCPDS NO. 04-0836).

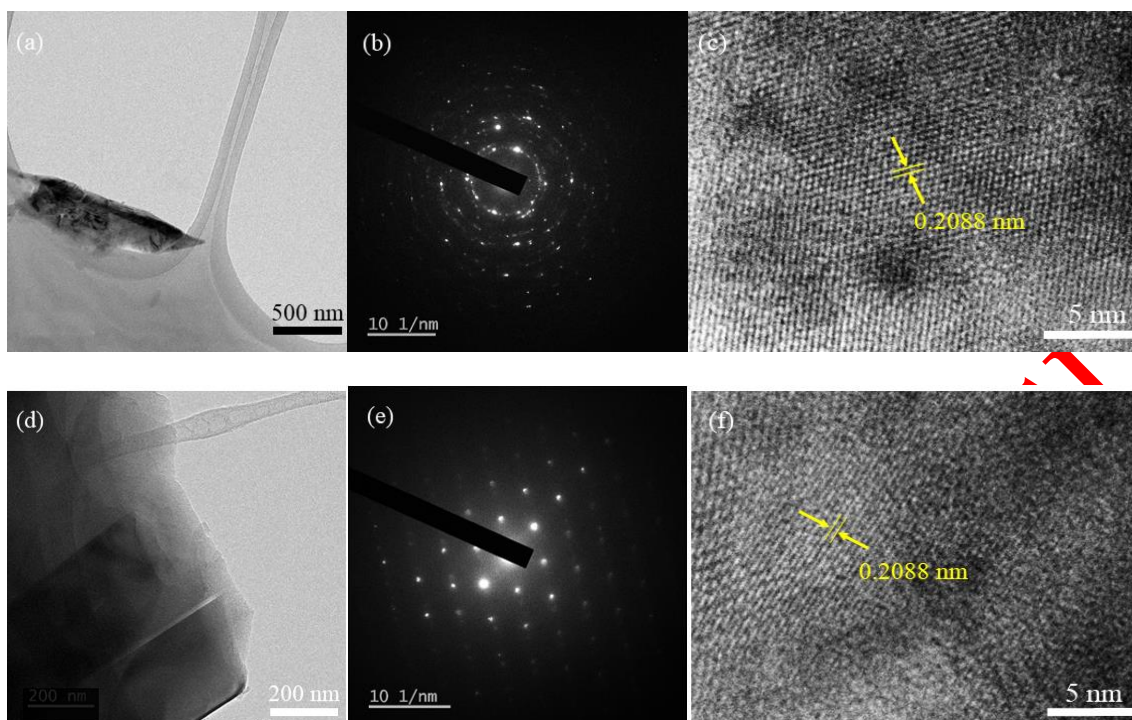


Fig. 4. TEM characterizations of dendritic and flower-like Cu particles.

Fig. 5 presents the Raman spectra of pure R6G powder and the same weight of R6G mixing with leaf-like and flower-like Cu particles under 532 nm in the range of  $500\text{ cm}^{-1}$  -  $1800\text{ cm}^{-1}$ . The peaks have been enhanced compared with pure R6G powder, but there are also some obvious differences in enhancement effect of them. The sample mixed with flower-like Cu particles has the higher degree of enhancement due to existence of more nanosheets and smaller size.

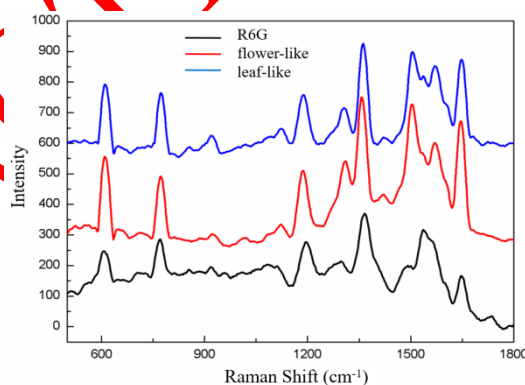


Fig.5. SERS spectrums of leaf-like and flower-like Cu particles.

### 3.2. Distribution-controlled analysis

Distribution-controlled Cu crystals deposited on substrates are illustrated in SEM images to analyze the controlled distribution (Fig.6). In Fig.6a, three protruding islands (the area with 20, 30 and 40  $\mu\text{m}$  width of defects, enclosed by red dashed line) are observed on the surface of the electrodeposited layer, showing the island-controlled distribution on substrates. Fig.6b shows one clear boundary of the slender island in Fig.6a. Cu crystals of different sizes grew on two areas, and the crystals in the same area had uniform distribution and similar morphology. The defected area on the island has a larger particle size, indicating that the defects promotes the growth of crystals.

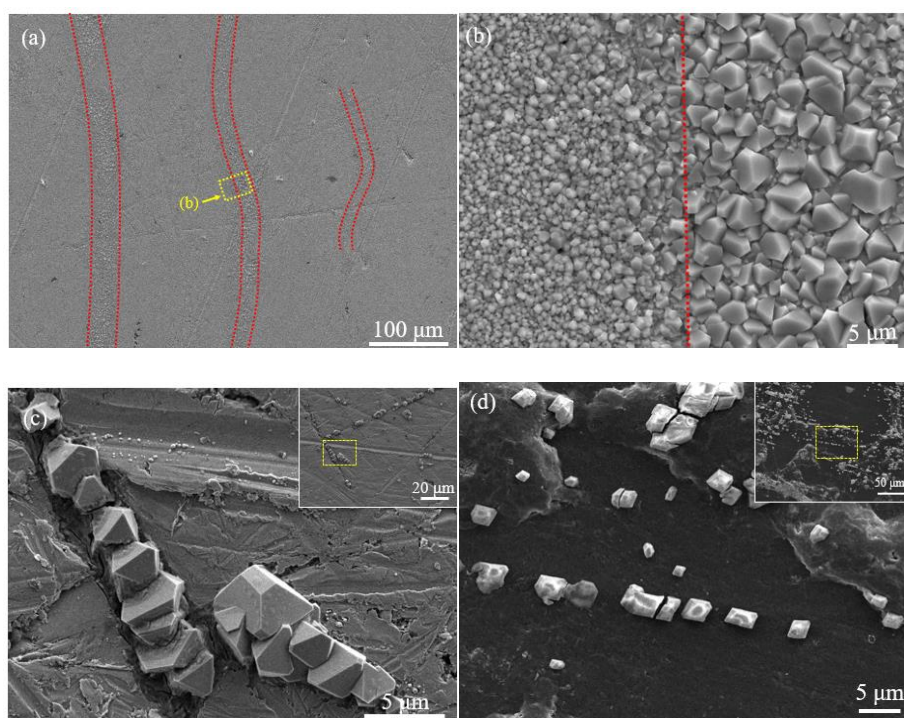


Fig. 6. SEM images of area-controlled growth of Cu and Ni crystals, (a) and (b) island-growth of Cu; (c) linear-growth of Cu; (d) linear-growth of Ni.

Furtherly, as the width of defects reduced to 5  $\mu\text{m}$ , a more obvious linear-controlled selective electrodeposition appeared: Cu crystals grew only in some defected areas of the substrate (Fig.6c). In order to further understand this growth behavior, the electrodeposition of Ni with the same conditions were examined (Fig.6d). Interestingly, under the same environment and substrate treatments (introducing defects of 5  $\mu\text{m}$ ), Ni crystals were also successfully found growing along linear defects in some area.

These experiments furtherly indicate that the defects introduced some factors which could accelerate  $\text{Cu}^{2+}$  and  $\text{Ni}^{2+}$  to nucleate and grow in the defected area, and even inhibit the nucleation in other areas. It inspires us the growth method of large single crystal metal particles during the electrodeposition process and makes the patterned fabrication of Cu film in additive manufacturing possible, compared with the previous patterned printing method by controlling the movement of the micropipette.

For a complete view of the formation process, Cu crystals in defected area under electrodeposition for 1 s were used to gain additional insight into the growth in early stage. In Fig. 7a and b, TEM observations for pieces of typical electrodeposited Cu clarify the presence of nanocrystals with the size of 5~10 nm (clear crystal profiles exist on the peeled substrate pieces) on the thin substrate piece, which show the finer scale microstructural features on the deposition surface of substrates. For the initial part such nanocrystals appear to be well fitted to explain the initial nucleation of Cu crystals at possible active sites induced by defect area aforementioned in Fig. 6.

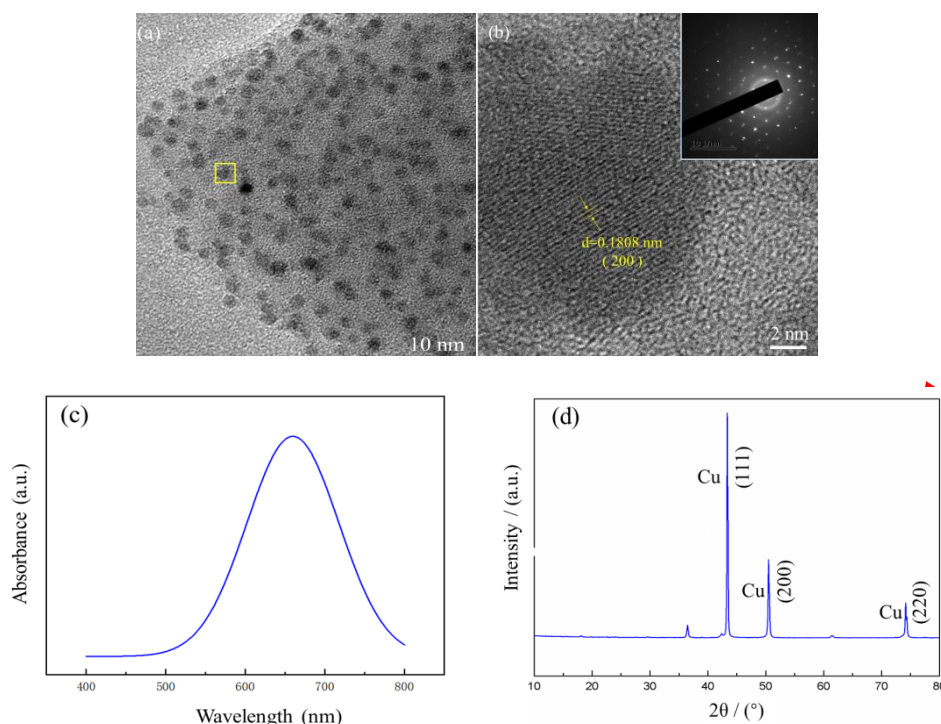


Fig. 7. TEM characterizations, UV-Vis and XRD spectra of Cu crystals.

Fig. 7b shows Cu nanocrystals in high resolution mode and demonstrate the regular lattice planes of 1.808 Å is consistent with the (200) plane of FCC Cu (JCPDS NO. 04-0836). SAED pattern at the top right can be indexed to FCC Cu (JCPDS NO. 04-0836). The symmetrical diffraction spots indicate the presence of single crystals. UV-Vis and XRD analysis Fig. 7c and d verify that the synthesized products are Cu crystals. The identified Cu peaks at 43.2°, 50.3°, and 74.1° are for the indices of (111), (200), and (220) respectively (JCPDS NO. 04-0836).

As mentioned above, there were high nucleation density along defected areas at early stage, with continued growth, all nuclei grow into polyhedral crystals with a diameter of micron, resulting in larger Cu crystals in the defected areas, or even growing only in defected areas.

#### 4. Conclusion

Leaf-like, dendritic, flower-like, multi-corner and multi-edge are obtained in a simple electrodeposition by changing substrates, temperature or introducing ultrasonic vibration, without template and surfactant. These particles have more distinctive bionic features than those reported, endowing Cu materials with intriguing properties such as an increased surface area and active site for SERS. Island- and linear-controlled growth due to different width of defects on substrate in the process of Cu crystal electrodeposition were studied. The linear-controlled growth was further confirmed by electrodepositing Ni crystals. The formation of Cu nanocrystals nuclei during the early stage of deposition was also studied. These reports not only provide valuable information for the study of electrochemical crystal growth mechanisms but also inspire growing large polyhedral single crystals and printing patterned conductive metal film in additive manufacturing.

#### Acknowledgements

The authors acknowledge financial support from the National Natural Science Foundation of China (Grant Nos. 51801138 and 51727901).

## References

- [1] N. Nikolic, P. Zivkovic, M. Pavlovic, Z. Bascarevic, J. Serb. Chem. Soc. **84**, 1209 (2019).
- [2] R. K. Nekouei, F. Rashchi, A. A. Amadeh, Powder Technol. **237**, 165 (2013).
- [3] Y. Lv, M. Liu, Surf. Eng. **35**, 542 (2019).
- [4] Suxiang Ge, Yange Zhang, Baojun Huang et al., Materials Letters **163**, 61 (2016).
- [5] N. D. Nikolic, K. I. Popov, Lj. J. Pavlovic et al., Journal of Electroanalytical Chemistry **588**, 88 (2006).
- [6] Ming Luo, Aleksey Ruditskiy, Hsin-Chieh Peng et al., Adv. Funct. Mater. **26**, 1209 (2016).
- [7] X. J. Zhang, G. F. Wang, X. W. Liu, H. Q. Wu, B. Fang, Crystal Growth and Design **8**, 1430 (2008).
- [8] W. Wu, R. Liang, L. Lu, W. Wang, X. Ran, D. Yue, Surf. Coat. Technol. **393**, 125744 (2020).
- [9] J. Liu, X. Huang, Y. Li, Z. Li, Q. Chi, G. Li, Solid State Sciences **10**, 1568 (2008).
- [10] Quang Duc Truong, Masato Kakihana, Journal of Crystal Growth **348**, 65 (2012).
- [11] Carl C. Koch, Nanostructured Materials: Processing, Properties and Applications (second ed.), William Andrew Publishing, New York, 521 (2006).
- [12] K. I. Popov, S. S. Djokić, N. D. Nikolić, V. D. Jović, Morphology of Electrochemically and Chemically Deposited Metals. Springer: New York, NY, USA, 1 (2016).
- [13] G. Orhan, G. Hapci, Powder Technol. **201**, 57 (2010).
- [14] M. G. Pavlović, L. J. Pavlović, V. M. Maksimović, N. D. Nikolić, K. I. Popov, Int. J. Electrochem. Sci. **5**, (18622010).
- [15] R. K. Nekouei, F. Rashchi, A. A. Amadeh, Powder Technol. **237**, 165 (2013).
- [16] W. Lou, W. Cai, P. Li, J. Su, S. Zheng, Y. Zhang, W. Jin, Powder Technol. **326**, 84 (2018).
- [17] Manila Mallik, Arijit Mitra, Srijan Sengupta, Cryst. Growth Des. **14**, 6542 (2014).
- [18] Yanling Wang, Liyan Zhao, Yu Zhao, Adv. Mater. **30**, 1805686 (2018).
- [19] Guannan Yang, Xian Zeng, Pengyu Wang, ChemElectroChem. **8**, (8192021).
- [20] S. Mahima, C. Karthik, S. Garg, R. Mehta, R. Teki, N. Ravishankar, G. Ramanath, Crystal Growth and Design **10**, (39252010).
- [21] Yonghong Ni, Yongmei Zhang, Jianming Hong, Crystal Growth & Design **11**, 2142 (2011).
- [22] M. Palomar-Pardavé, E. Garfifias-García, M. Romero-Romo, Electrochimica Acta **56**, 10083 (2011).
- [23] Lian Guo, Peter C. Searson. Nanoscale **2**, 2431 (2010).
- [24] Lian Guo, Gerko Oskam, Aleksandar Radisic, J. Phys. D: Appl. Phys. **44**, 443001 (2011).
- [25] Lian Guo, Peter C. Searson. Langmuir **24**, 10557 (2008).
- [26] S. J. Stranick, M. M. Kamna, P. S. Weiss, Nanotechnology **7**, 443 (1996).
- [27] Mark Aarts, Stefan van Vliet, Roland Bliem, CrystEngComm. **23**, 3648 (2021).
- [28] F. Nasirpour, S. J. Bending, L. M. Peter, H. Fangohr, Thin Solid **519**, 8320 (2011).
- [29] Taekyung Yu, Zhaohui Wu, Woo-Sik Kim, RSC Adv. **4**, 37516 (2014).